Joining $MoSi_2$ to 316L stainless steel

S. D. CONZONE, D. P. BUTT, A. H. BARTLETT
Materials Science and Technology Division, Los Alamos National Laboratory, Los Alamos, NM 87545, USA

The feasibility of joining $MoSi_2$ to 316L stainless steel using active brazing techniques was investigated using two interlayer systems: cusil/Nb/cusil and cusil/Ni/cusil (where cusil is a commercially available Cu–Ag eutectic). Dense, uniform joints were obtained with the cusil/Nb/cusil interlayer system, because the coefficient of thermal expansion (CTE) of niobium closely matched that of $MoSi_2$ over a wide temperature range. Matching the CTEs of $MoSi_2$ and the interlayer material shielded the low-toughness $MoSi_2$ from residual stresses formed during cooling from the joint-processing temperature (830 °C). The cusil/Ni/cusil interlayer, however, failed to produce adequate joints because of the large CTE difference between nickel and $MoSi_2$.

1. Introduction

Molybdenum disilicide ($MoSi_2$) has great potential as a high-temperature structural material, owing to its excellent oxidation resistance, high melting temperature, good electrical conductivity, relatively low coefficient of thermal expansion (CTE), a brittle to ductile transition near 1000 °C, and stability in a variety of corrosive environments [1–5]. Some potential uses for $MoSi_2$ include furnace components, gas burners and ignitors, high-temperature filters, gas injection tubes, and high-temperature nozzles [1, 6].

In order for $MoSi_2$ to be used in many of the aforementioned applications it must first be joined to other materials, such as ferrous and non-ferrous alloys. However, direct bonding of $MoSi_2$ to most metals is not possible owing to differences in CTE and the necessity for high joining temperatures, which can lead to joint failure upon cooling because of large residual stresses. Low-temperature brazing techniques and the use of ductile interlayers of intermediate CTE can reduce these thermal stresses developed upon cooling from the bonding temperature.

This is the first published work to examine the joining of $MoSi_2$ to a dissimilar material. Niobium and nickel were used as ductile intermediate layers. Joining was achieved at moderate temperatures by traditional active brazing techniques using a copper–silver eutectic (Cusil™, Wesgo Inc., Belmont, CA 94002) as the brazing medium.

2. Experimental procedure

$MoSi_2$ powder was obtained commercially (Cerac, Inc., Milwaukee, WI 53201) and hot pressed into billets with densities $>95\%$ theoretical. 316L L stainless steel was obtained in the form of discs with a diameter of 15.8 mm and a thickness of 2.4 mm (Metal Samples, Inc., Munford, AL 36268). Foils, 125 μm thick, of 99.9% pure nickel and niobium were obtained commercially (Aldrich Chemical, Inc., Milwaukee, WI 53233). Copper/silver eutectic foil (50 μm thick) was purchased and subsequently rolled down to 20 μm.

A diamond wafering saw was used to cut 5 mm × 5 mm × 3 mm rectangular bonding specimens from the hot-pressed billets of $MoSi_2$. These $MoSi_2$ specimens were polished to 1 μm diamond finish using standard metallographic techniques. The niobium, nickel, and cusil foils were cut into 5 mm × 5 mm squares using steel shears. The $MoSi_2$ samples, foils and as-received steel discs were then ultrasonically cleaned in acetone followed by deionized water. After cleaning, all samples were allowed to dry at 150 °C for 5 min.

Bonding was achieved using the block/interlayer/block assembly shown in Fig. 1. After arranging

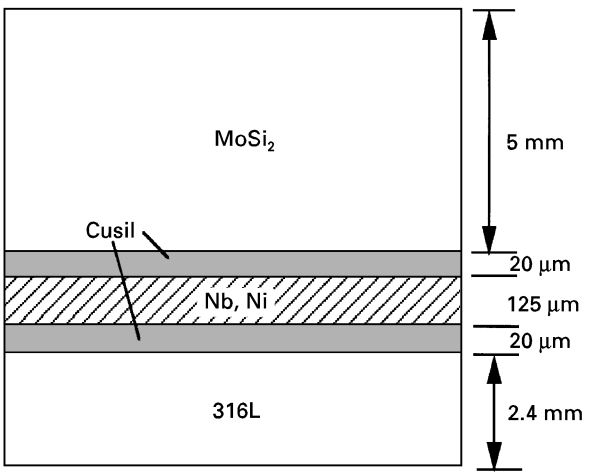

Figure 1 Pictorial representation of the block/interlayer/block assembly used during joining.

0022–2461

the foils and bonding specimens in the block/interlayer/block orientation, the entire assembly was placed into a loading device composed of two Al_2O_3 plates and four Al_2O_3 bolts. The Al_2O_3 press applied a stress of approximately 10 MPa during bonding to ensure sufficient contact. The loaded Al_2O_3 press was placed into a tube furnace which was vacuum purged with ultra-high-purity Ar–6% H_2 gas (three times) at room temperature and again at 250 °C to remove oxygen and absorbed water from the furnace and bonding assembly. The ultra-high-purity Ar–6% H_2 gas was gettered by passing it first through calcium sulphate at room temperature and then 99.9% pure copper at 650 °C. A ramp rate of 5 °C min^{-1} was used to heat the furnace to the joining temperature of 830 °C (50 °C above the 780 °C cusil eutectic). The temperature was then held at 830 °C for 10 min before cooling at 2 °C min^{-1} to room temperature. Gettered Ar–6% H_2 gas was continuously leaked through the furnace during the ramp and hold cycles. After bonding, the specimens were characterized by scanning electron microscopy (SEM) and electron probe microanalysis (EPMA).

In addition, 316L/Nb/$MoSi_2$ joints, 10 mm × 10 mm × 25 mm in size, were made in order to obtain mechanical test specimens. After joining, beams of approximate dimension 2 mm × 2 mm × 25 mm were cut by electro-discharge machining from the joint. The tensile face of the beam was ground to a 600 grit finish, and the edges were bevelled to prevent corner failures during mechanical testing. Four-point bend tests of the joined specimens were done at room temperature at a strain rate of 10^{-4} s^{-1}. Fracture surface and crack path analysis were conducted post-test.

3. Results and discussion

3.1. Residual stress analysis

A low-magnification scanning electron micrograph of a joint produced using a cusil/Nb/cusil interlayer is shown in Fig. 2. The cusil/Nb/cusil interlayer system produced a joint with no cracking or porosity. Fig. 3 shows the cusil/Ni/cusil joint. In contrast, the nickel interlayer system produced a joint with a porous interface and catastrophic cracking through the $MoSi_2$. Cracking initiated at the free surface of the $MoSi_2$, a few micrometres from the interface. The cracks appeared to travel parallel to the interface for ~10 μm, then turned towards and travelled a significant distance in the $MoSi_2$ (the lower modulus material), and eventually propagated parallel to the interface. It should be noted that we have joined $MoSi_2$ to 304L using much thicker (≈500 μm) layers of nickel under otherwise similar conditions.

The occurrence of cracking in joints is a result of large stresses developing due to CTE mismatch between the materials being joined. Plastic deformation within the interlayer of a joint is one mechanism that can partially relieve these stresses. Because the extent of stress relaxation is directly related to the yield strength, σ_y of the interlayer materials, indentation testing was performed on the nickel and niobium materials in the joints at temperatures ranging from room temperature to 800 °C, in order to obtain σ_y data [7]. Fig. 4 plots σ_y as a function of temperature, indicating σ_y of nickel is less than that of niobium over the entire temperature range. Apparently, simple stress relaxation by plastic deformation of the interface is not a sufficient explanation for the absence of cracking in the niobium joint as compared to the catastrophic failure of the nickel joint. Therefore,

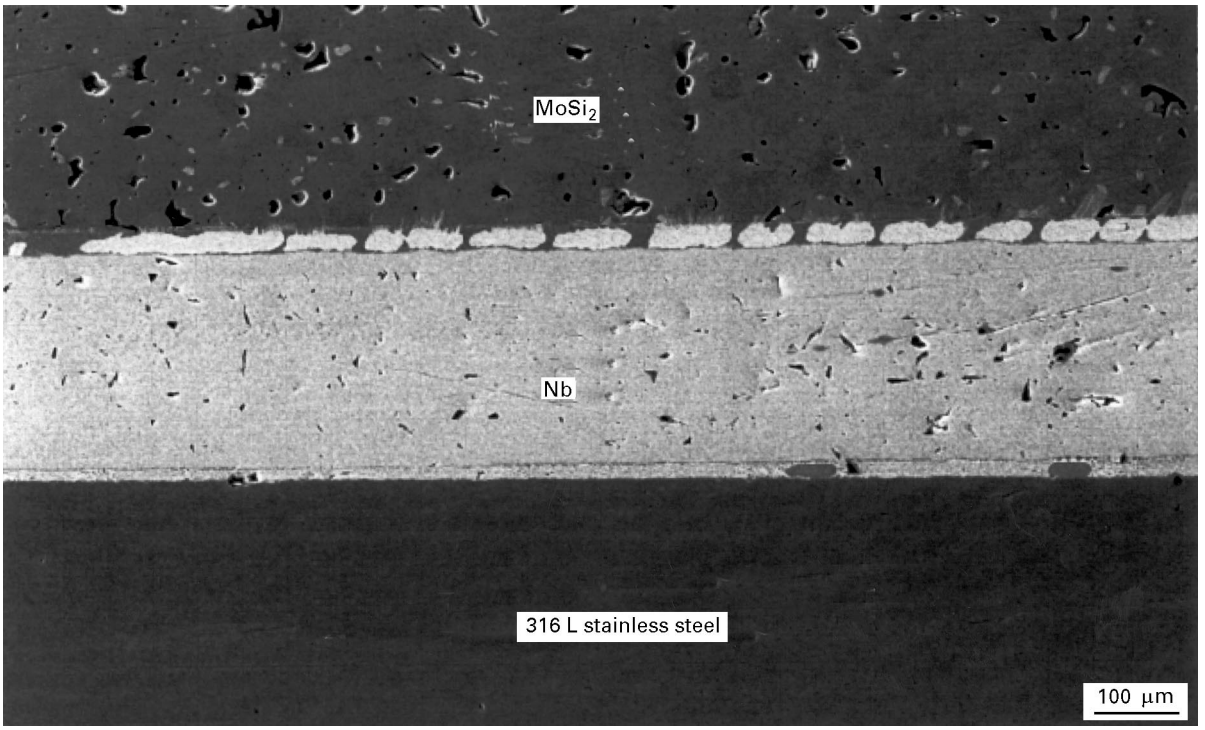

Figure 2 Low-magnification, secondary electron scanning electron micrograph of a $MoSi_2$/316L joint formed using a cusil/Nb/cusil interlayer.

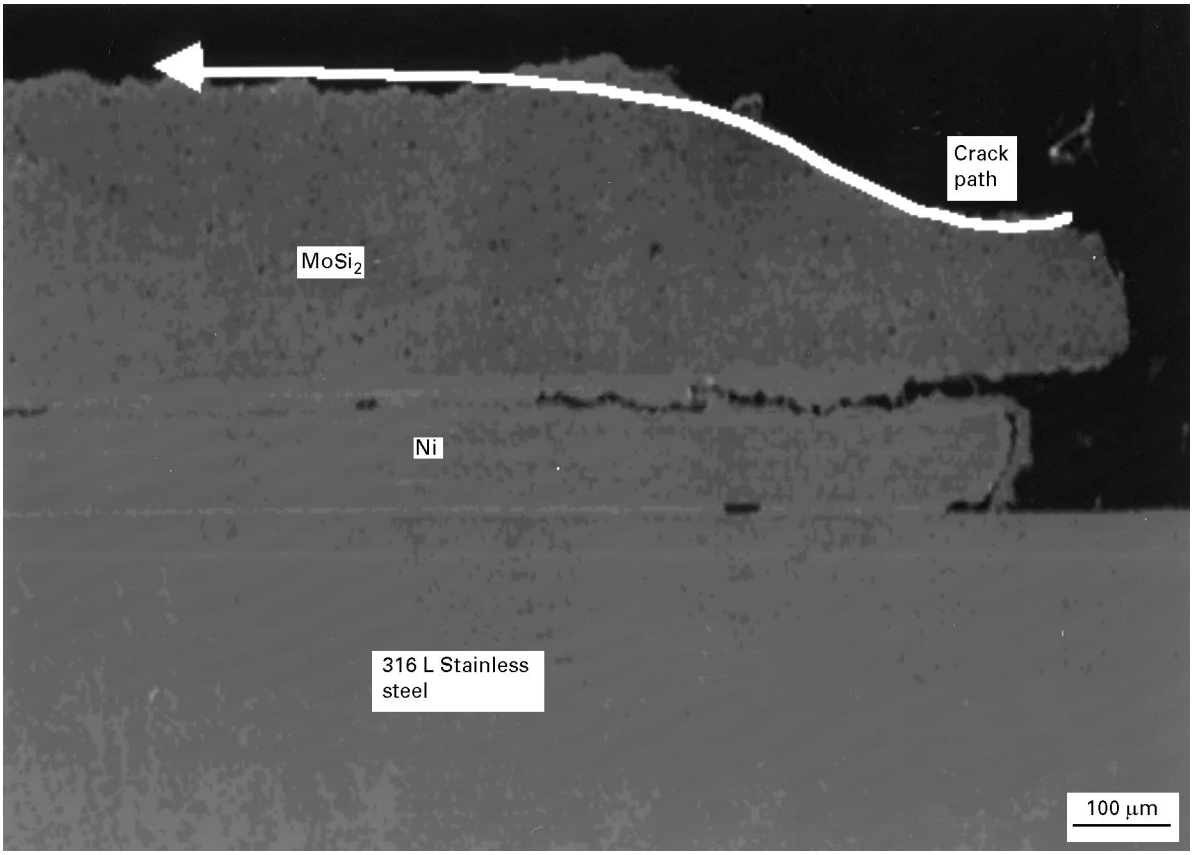

Figure 3 Low-magnification, secondary electron scanning electron micrograph of a $MoSi_2$/316L joint formed using a cusil/Ni/cusil interlayer. Note that the cracking initiated at the free surface, adjacent to the interface, and then propagated parallel to the interface entirely through the $MoSi_2$.

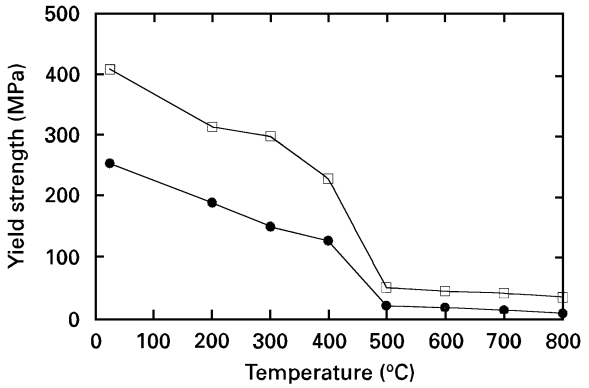

Figure 4 Yield strength of (□) niobium and (●) nickel foils as a function of temperature.

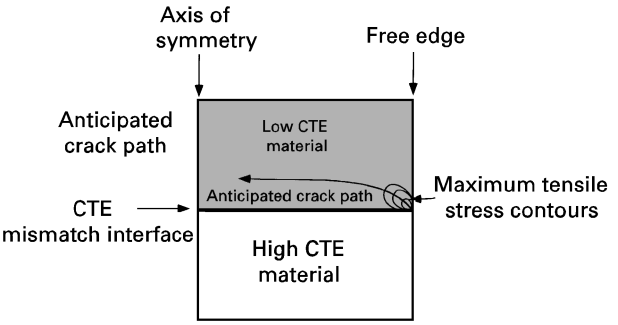

Figure 5 The two-region system modelled by Drake *et al.* [9] using finite element analysis. Note that the maximum tensile stress contours exist at the free surface of the low-expansion material, in close proximity to the interface.

in addition to the magnitude of the stresses, their location and orientation must also be considered. According to finite element analytical models and experimental findings [8–13], tensile axial stresses form near the free surfaces of the low-expansion material, adjacent to the interface, during cooling, when joining materials of dissimilar CTEs. A pictorial representation of these stresses, and predicted residual stress-driven crack paths, is given in Fig. 5 [12]. Because nickel and the 316L have similar CTEs (Fig. 6), tensile stresses were likely concentrated in the $MoSi_2$, adjacent to the Ni/$MoSi_2$ interface, during cooling. These tensile stresses led to cracking and failure through the low-toughness $MoSi_2$. Conversely, the absence of cracking when using the niobium interlayer system can be rationalized by noting the location where CTE mismatch stresses were maximized. In this system, tensile stresses would be expected to be concentrated in the niobium foil (adjacent to the 316L/Nb interface) during cooling. The low yield strength and high toughness of the niobium relieved residual stresses and prevented crack extension while shielding the low-toughness $MoSi_2$ from tensile stresses.

3.2. Mechanical testing

Four-point bend tests showed linear strains to failure. Four samples were tested, with an average failure

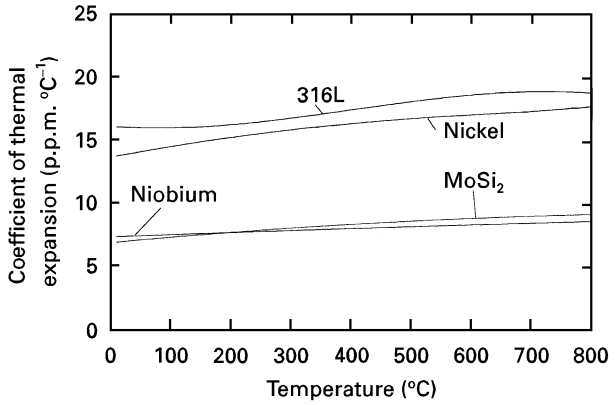

Figure 6 Thermal expansion coefficient (CTE) of 316L stainless steel, $MoSi_2$, niobium and nickel.

strength of 85 MPa. Failure typically appeared to initiate in the silicide, and propagated along a path parallel to, and approximately 10 μm from, the interface (Fig. 7). Typical strength values for hot-pressed $MoSi_2$ of this quality are in the range of 400 MPa. Because the strength of the joined specimens is effectively limited by the strength of the $MoSi_2$, residual axial tensile stresses are responsible for reducing the strength of the bond below the intrinsic strength of the $MoSi_2$. For instance, using the formulation of Suganuma *et al.* [14] for joined cylinders, residual tensile stresses of approximately 900 MPa could be expected at the $MoSi_2$ free surface. This analysis does not take into account reductions in stress due to plasticity of the metal, but serves to illustrate that large residual stresses are an inherent part of the joining process and will reduce the measured strength of the joints. Cracking parallel to the interface is often seen in joints of dissimilar materials [15]. Plasticity of the interlayer [16] and relative toughnesses of the interface and the silicide [17] all favour cracking in the $MoSi_2$, though details such as the distance from the interface at which the crack propagates, and the above contributions to fracture energies, cannot be predicted.

3.3. Chemical analysis

Higher magnification scanning electron micrographs of the diffusion zones produced at the 316L/Nb and $MoSi_2$ /Nb interfaces are given in Figs 8 and 9, respectively. The diffusion zones shown in Figs 8 and 9 are relatively small ($\approx$10 μm) and are composed of several phases. Electron probe microanalysis (EPMA) was used to identify each of the phases present at the two interfaces. Chemical analysis was not performed on the nickel bond shown in Fig. 3 because catastrophic cracking and large amounts of porosity make that bond inappropriate for most applications.

Two major phases were present at the 316L/Nb interface shown in Fig. 8. Gross segregation of the cusil eutectic during the bonding caused the

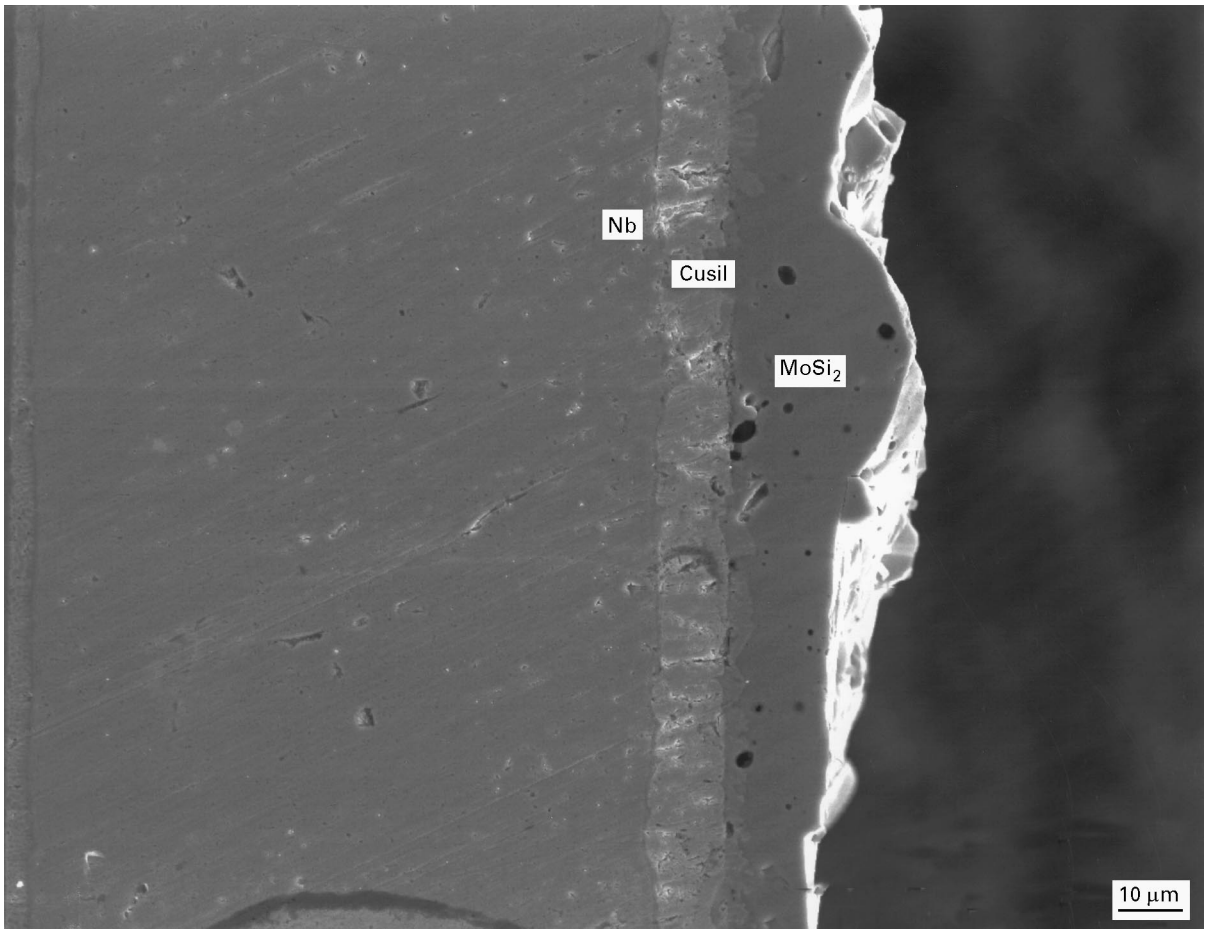

Figure 7 Crack path in $MoSi_2$/Nb/316L joint after four-point bending.

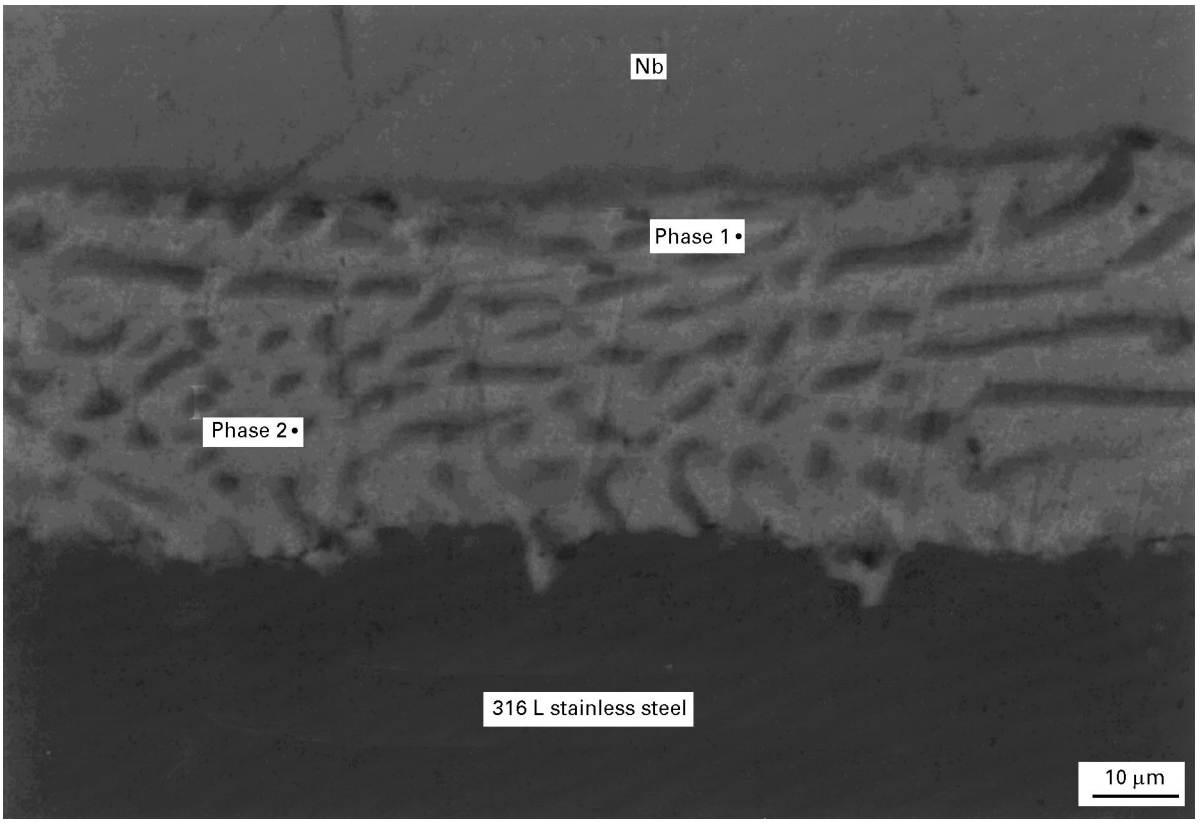

Figure 8 Secondary electron scanning electron micrograph of the 316L/Nb interface.

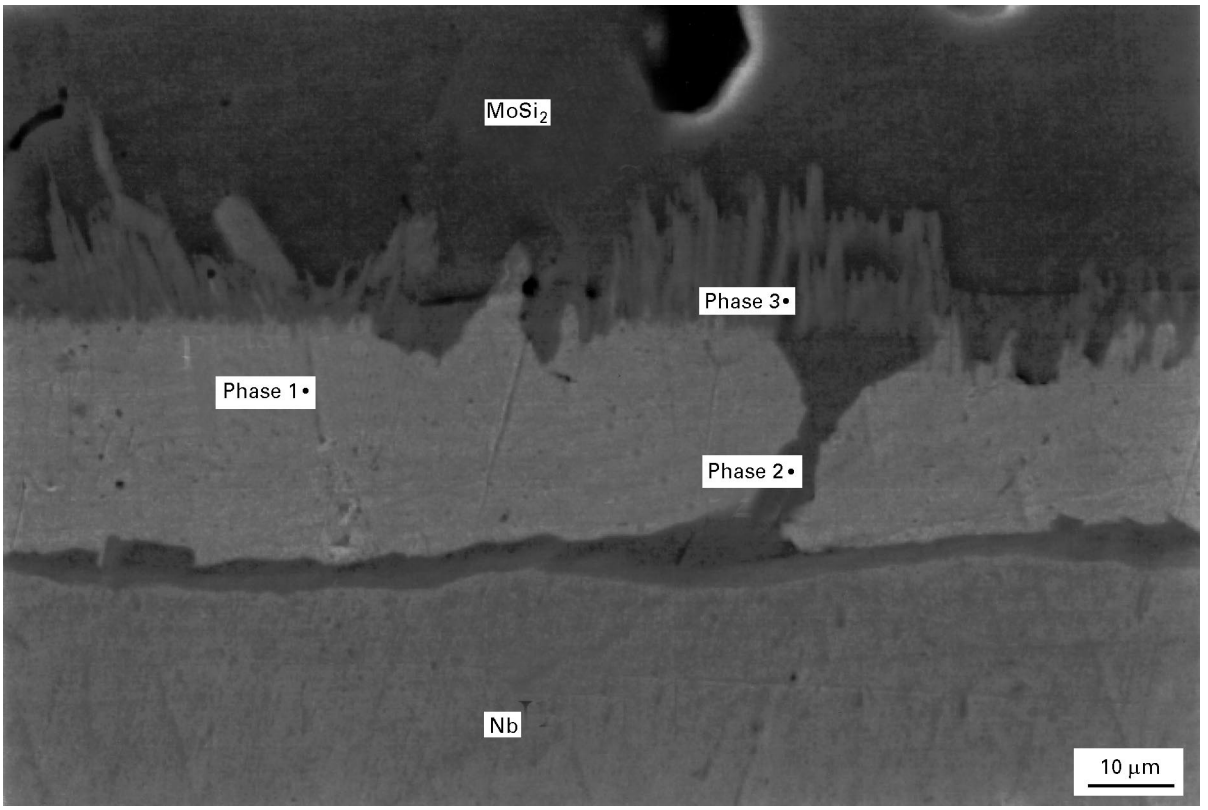

Figure 9 Secondary electron scanning electron micrograph of the $MoSi_2$/Nb interface.

formation of two Ag/Cu alloys rich in either silver (Phase 1) or copper (Phase 2). These silver (92–94 at %) rich and copper (96–98 at %) rich alloys have approximate melting temperatures of 925 and 1070 °C, respectively.

There were three major phases formed at the $MoSi_2$/Nb interface shown in Fig. 9. As with the 316L/Nb interface, gross segregation of the cusil eutectic composition during bonding caused the formation of Phase 1, a Cu/Ag alloy composed of

92–94 at % Ag. Phase 2 was determined to be a Cu/Si phase composed of 88–90 at % Cu. This Cu/Si phase is a peritectic composition with a melting point of 852 °C. Phase 3 was determined to be Mo_5Si_3. Mo_5Si_3 phase formed near the interface as silicon diffused out of the pure $MoSi_2$ to form the Cu/Si phase. Mo_5Si_3 is a refractory phase which has a melting temperature of 2180 °C.

The melting temperature of the Cu/Si peritectic phase (852 °C) is the lowest of any phase identified. Because the use temperature of a joint is limited by the melting temperature of the least refractory phase, the niobium joint produced cannot be used at temperatures approaching or exceeding approximately 850 °C.

4. Conclusion

Two interlayer systems were used to join $MoSi_2$ to 304L stainless steel: cusil/Nb/cusil and cusil/Ni/cusil. Successful $MoSi_2$/316L joints were produced when the niobium interlayer system was used; however, cracking in the $MoSi_2$ was observed when using the nickel system. The niobium system was successful in producing a crack free joint because niobium has a CTE which closely matches that of $MoSi_2$. Matching the CTEs of $MoSi_2$ and the interlayer allowed residual stresses to be concentrated within the high-toughness interlayer, shielding the $MoSi_2$ from tensile stresses. Although an interlayer thickness of approximately 125 μm was used in this study, the optimal interlayer thickness which would provide shielding from CTE mismatch stresses while still yielding high strength values is not known.

The reaction zones produced at the two cusil interfaces were minimal in size and could be further decreased using thin films rather than foils. Foils were utilized in this study to prove the feasibility of using solely commercially available materials and a relatively simple experimental procedure to obtain $MoSi_2$/316L joints. The Cu/Si phase produced at the $MoSi_2$/Nb interface limits the use temperature of $MoSi_2$/316L joints because it has a relatively low melting temperature (852 °C). It should be noted that the successful use of this joint at temperatures approaching 852 °C could only be achieved in a non-oxidizing environment.

These results indicate that it is possible to obtain $MoSi_2$/316L stainless steel joints at low processing temperatures when interlayer systems with CTE behaviour similar to that of $MoSi_2$ are utilized. Future work will be concentrated in four major areas;

1. determining the optimal interlayer thickness for joint strength and tensile stress shielding;
2. using other liquid-phase formers (such as pure silver) in an attempt both to minimize reaction at the interface and increase the refractoriness of the final joint;
3. attempting to replace niobium with oxidation-resistant alloys which have CTE behaviour similar to $MoSi_2$ (such as Ni–Fe alloys), in an attempt to increase the use temperature of $MoSi_2$/316L stainless steel joints in oxidizing environments;
4. joining $MoSi_2$ to nickel-based superalloys and other commercially available alloys.

Finally, it should be noted that the magnitude of the residual stress in any joint is strongly affected by the size and shape of the specimen. It has been demonstrated [8, 18] that increasing the height or width of a joining specimen will also increase the axial stresses developed in the lower CTE material during cooling. Thus, in evaluating other $MoSi_2$/316L joints, careful consideration must be given not only to the CTEs of the materials, but also to specimen geometry.

Acknowledgements

This work was supported by the US Department of Energy, Advanced Industrial Materials Program. The authors are grateful to our DOE program managers, Charles Sorrell and Suzane Leonard. We are also grateful to John Petrovic and Rich Castro of Los Alamos National Laboratory for helpful discussions and for supplying some of the materials used in these studies.

References

1. J. J. PETROVIC, *MRS Bull* **18** July (1993) 35.
2. J. J. PETROVIC and J. S. IDASETIMA, *Mater. Res. Soc. Symp. Proc.* **322** (1995) 107.
3. T. C. CHOU and T. G. NIEH, *J. Mater. Res.* **8** (1993) 214.
4. D. A. BERZTISS, R. R. CERCHIARA, E. A. GULBRANSEN, F. S. PETTIT and G. H. MEIER, *Mater. Sci. Eng.* **A155** (1992) 165.
5. J. J. PETROVIC, *ibid.* **A192–193** (1995) 31.
6. A. BARTLETT, R. CASTRO, H. KUNG, D. P. BUTT and J. J. PETROVIC, *Ind. Heating J. Thermal. Tech.* **63** (1996) 33.
7. P. J. BLAU and B. R. LAWN, "Microindentation Techniques in Materials Science and Engineering" (American Society for Testing and Materials, Philadelphia, PA, 1985) p. 146.
8. R. L. WILLIAMSON, B. H. RABIN and J. T. DRAKE, *J. Appl. Phys.* **74** (1993) 1310.
9. J. T. DRAKE, R. L. WILLIAMSON and B. H. RABIN, *ibid.* **74** (1993) 1321.
10. M. D. DRORY and A. G. EVANS, *J. Am. Ceram. Soc.* **73** (1990) 634.
11. M. D. DRORY, M. D. THOULESS and A. G. EVANS, *Acta Metall.* **36** (1988) 2019.
12. H. C. CAO, M. D. THOULESS and A. G. EVANS, *ibid.* **36** (1988) 2037.
13. A. BARTLETT, A. G. EVANS and M. RÜHLE, *Acta Metall. Mater.* **39** (1991) 1579.
14. K. SUGANUMA, T. OKAMOTO, M. KOIZUMI and M. SHIMADA, *J. Am. Ceram. Soc.* **68** (1985) C334.
15. J. W. HUTCHINSON, M. E. MEAR and J. R. RICE, *J. Appl. Mech.* **54** (1987) 828.
16. B. J. DALGLEISH, K. P. TRUMBLE and A. G. EVANS, *Acta Metall.* **37** (1989) 1923.
17. A. G. EVANS, B. J. DALGLEISH, M.-Y. HE and J. W. HUTCHINSON, *ibid.* **37** (1989) 3249.
18. K. SUGANUMA, T. OKAMOTO, M. KOIZUMI and M. SHIMADA, *J. Am. Ceram Soc.* **68** (1985) C334.

Received 25 July
and accepted 23 October 1996